RSC Advances

ROYAL SOCIETY OF CHEMISTRY

www.rsc.org/advances

Graphical image

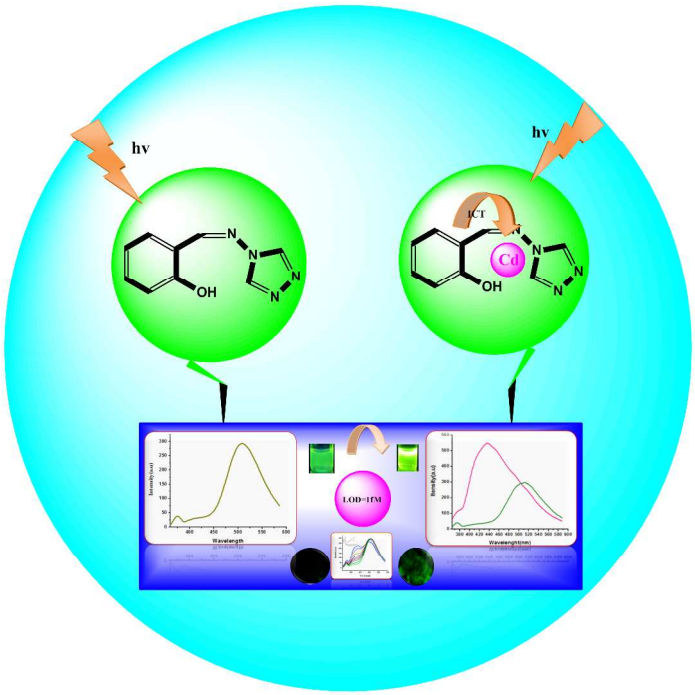

A Simple Highly Sensitive and Selective TURN-ON Fluorescent Chemosensor for the Detection of Cadmium Ions in Physiological Condition

Sundaram Ellairaja[a], Ramar Manikandan[b], Muthunanthevar Vijayan[c], Seenivasan Rajagopal[a], Vairathevar Sivasamy Vasantha[a]*

[a] School of Chemistry, Madurai Kamaraj University, Madurai-625021, Tamilnadu, India.

[b] University of Madras, Chennai-600035, Tamilnadu, India.

[c] Central Electro Chemical Research Institute, Karaikudi, Tamilnadu, India.

*Corresponding Author

Email id: vasantham999@yahoo.co.in (V. S. Vasantha)

Tel: 91-452-2458246; Fax: 91-452-2459139

Abstract

A very simple fluorophore was synthesized and applied as chemosensor for Cd^{2+} ions detection. Structural characterization was done by ^{1}HNMR ^{13}C and ESI-Mass techniques. All the fluorimetric titrations were carried out by using spectrofluorimetriy. The fluorophore has showed a very good with LOD of 1 fM towards Cd^{2+} ions. The linear range of detection is 5 fM^{-1} to 1mM. Moreover, it has successfully discriminate Zn^{2+} ions and all interfering metal ions in physiological pH (7.5). The quantum yield of the fluorophore increased from 0.4 to 0.78 after the binding of Cd^{2+} ions .The formation of 1:1 complex is confirmed by Job's plot, ^{1}H NMR and ESI-Mass which have strongly manifests the formation of 1:1 complex. The binding constant is also calculated for the probe-Cd^{2+} ions in lower (femto) concentrations as 2.2 $x10^{3}$ M^{-1}.The chemosensor has also exhibited very good results in He-La Cells imaging under physiological pH. So the chemosensor that has developed can be recommended for the practical biological applications especially in oncology.

Keywords: Chemosensors, Internal Charge Transfer, Discrimination, Turn ON, Cell imaging

Introduction

Design of a metal ion sensor has been allured through many researchers related to various applications such as clinical toxicology, environmental bioinorganic chemistry, bioremediation, and waste management.[1-3] There were so many sensors have been developed for different metal ions since from the last 10 decades. The need for the development of metal sensor has been increasing till now for their peculiar sensitivity in order to applications concern. Among various metal ions Cd^{2+} ions, is highly noticed due to its high toxicity and carcinogenicity. Cadmium, whose half-life in humans is estimated to be between 15 and 20 years is listed by the U.S. Environmental Protection Agency as one of 126 priority pollutants. Cadmium was listed a number 7 on ATSDR's "CERCLA Priority List of Hazardous Substances". In addition, it can accumulate in the human body for >10 years.[4] The extensive use of cadmium metal in industrial and agriculture fields lead to water and soil contamination. Cadmium ions contamination is mainly derived from phosphate fertilizers, metal alloys, Ni-Cd batteries, paint pigments, ceramic enamels and natural factors like erosion, abrasion and volcanic eruption.[5] The intake of cadmium

ions by the cells has showed an adverse effect in cellular functions, molecular mechanism and causes so many acute health diseases like lung cancer, kidney cancer, renal cancer and prostate cancers**.** Smoking and inhalation of cadmium-containing dust represent additional sources of cadmium uptake in humans. Cadmium ions accumulation is involved in neurological, reproductive, cardiovascular, and developmental disorders.[6] Even the fertility of the soil is affected primarily with cadmium ions contamination which leads to the poor growth of corps.

In order to quantification of cadmium ions, numerous high cost and sophisticated methods were available such as inductively coupled atomic plasma mass spectroscopy (ICP-MS),[7] inductively coupled plasma emission spectroscopy (ICP-AES),[8] atomic absorption spectroscopy (AAS) and anode stripping voltammetry.[9] Amid these, the fluorescence spectral analysis has been used as a powerful analytical tool owing to its operational simplicity, cost effectiveness, high sensitivity and selectivity.[10] Many fluorescent sensors has been successfully developed for cadmium ions based on the mechanism like PET, ICT, CHEF, FRET etc.[11-12] But only a few of them are applicable to live cell imaging.[13] It is due to poor water solubility of probe, UV-excitation and pH-dependent fluorescence in physiological environments. However the need for developing the cadmium ion sensor in aqueous and biological media has been gradually increasing for its potential applications in living cell imaging. Besides, there is a challenge persisting till now in discriminating ability of the probe towards Zn^{2+} ions in selectivity point of view concern since these two metal ions are having similar physical and chemical properties. Hence, most of the developed sensors showed a poor selectivity between Cd^{2+} and Zn^{2+} ions. [14] In some cases, the fluorescence enhancement was achieved for probe after the addition of various nanomaterials like silver nanoparticles, quantum dots and graphene sheets.[15] But these type of nanoparticles based cadmium ions sensors are belonging to the hard matter.

Recently few chemosensors have been developed for distinguish the Cd^{2+} ions from Zn^{2+}ions with different mechanisms.[16-18] Amidst these, only a very few reports had showed a good discrimination for Cd^{2+}ions from Zn^{2+} ions.[19-20] Lu and co-workers had reported a selective ratiometric sensor for Cd^{2+}ions which were detected in neutral aqueous medium based on two different ICT mechanism.[21] By utilizing the unique role of 2-picolyl group, they demonstrated a new discrimination strategy for Cd^{2+} ions from Zn^{2+}ions with the LOD of 0.1μM. For the first time Peng and co -workers had developed Cd^{2+}ions sensor in water/acetone mixture which had showed a good discrimination of Cd^{2+} ions from Zn^{2+}ions and enhanced fluorescence intensity

with shift in emission using BODIPY (4,4-difluoro-1,3,4,5,7-quantmethyl-4- bora-3a,4a-diaza-*s*-indacene) as fluorophore.[22] Table.1 shows the different types Cd^{2+} ion sensors reported so far with their LOD. Keeping these points in mind, we have synthesized a very simple Schiff base ligand [(Z)-2-(4H-1, 2, 4-triazol-4-yl) imino methylphenol] as a probe and utilized successfully for the sensing of Cd^{2+} ions over Zn^{2+} ions. The developed fluoro sensor has showed a clear discrimination for Cd^{2+} ions towards Zn^{2+} ions when compare to the other sensors mentioned above. Besides, the sensor has showed a very good linear range of detection from5*f*M to 1*m*M with an excellent LOD of 1*f*M.

Experimental

Materials and general methods

Analytical grade solvents and double distilled water were used in all steps. The acetate salts of different metal ions were used. ^{1}H-NMR and ^{13}C-NMR were measured on a BrukerAV-400 spectrometer with chemical shifts reported in ppm (in $(CD_3)_2S=O$, or DMSO; TMS as internal standard). Mass spectra were measured on a Thermofleet LC-MS spectrometer. All pH measurements were made with a Eutek pH-Tutor. All the UV studies were done with JASCO 550 and Fluorescence spectra titrations were carried out with CARY Eclipse Fluorescence spectrophotometer. Fluorescence microscope (Model: LEICA DMLS) with an objective lens of 20 magnification was used for the cell imaging studies.

Synthetic route for the fluorophore

A solution of I (1.0 mL, 0.94 mmol, 1 equiv.) dissolved in absolute ethanol (10 mL) was added to a solution of II (1 equiv.) in ethanol (5 mL). The resulting slightly yellow solution was irradiated in microwave oven for 10 mins and the resulting pale-yellow solution was allowed to cool to room temperature to give a crystalline white powder III (Scheme 1). The product was filtered, washed with ethanol and diethyl ether and dried over $MgSO_4$ vacuum (2.5 g, 95%). The method of preparation was simple and fast as the totally 10mins was required for this synthesis, when compare to other previous reports.[27, 28] ^{1}H NMR (400 MHz, [D6] DMSO, 298 K): δ = 10.47 (s, 1 H), 9.18 (D, 2H), 7.80 (m, 1 H), 7.44 (m, 1 H), 7.02 (m, 2 H) ppm.(Fig. S1) ^{13}C NMR (400 MHz, [D6] DMSO, 298 K): δ = 158.57 (C9), 155.31 (C7), 139.43 (C3 and C5), 134.36 (C11), 128.13 (C13), 120.11 (C10), 118.65 (C8), 117.17 (C12) ppm.(Fig. S2) C9H8N4O (calculated mass 188.19): Observed Mass $[M+H]^-$ =187.09 (Fig. S3)

Result and Discussion

Optimization of pH for the Probe

In general the protons in probe/fluorophore determine the fluorescence response of the probe and the detection of metal ions, so it is necessary to investigate the effect of pH. Fig. 1 shows the fluorescence response of probe as a function of pH. Initially the probe showed an emission peak at 511 nm (Fig. 2b) which is mainly owing to the ICT mechanism. The donating nature of hydroxyl and imine functional groups are took part into this mechanism. From the optimization graph, it was clearly seen that under acidic conditions the functional groups in the fluorophore gets protonated. So the initial ICT mechanism is arrested. When the pH is increased from 1.0 to 7.0 there is a gradual increment in fluorescent intensity. This is mainly due to the gradual relaxation of arrested ICT mechanism. At pH 7.0, a maximum emission was observed due to the free hydroxyl and imine functional groups under neutral medium which initiates the ICT mechanism once again. Under this neutral aqueous media, in the ground state, the hydroxyl group promotes the electron transfer. When the pH is increased from 7.0 to 13.5, a decrease in fluorescence signal (excited at 332 nm) could be observed for the probe suggesting that deprotonation of hydroxyl group takes place. Meanwhile, the imine group gets protonated by absorbing this deprotonated hydrogen from the hydroxyl group. As a result, a gradual decrease in emission intensity is observed which mainly suggests the inhibition of ICT mechanism. No drastic change in wavelength shift is observed while varying the pH from 1 to 13.5. Under acidic condition (pH 1), the probe shows an emission peak at 501nm while the pH is adjusted from 2 to 6, the emission peak is slightly red shifted from 501 nm to 508 nm. Under neutral medium (pH 7), the probe gives its original fluorescence peak at 511 nm. When the pH is further varied from 8 to 13.5, the emission peak at 511 nm is blue shifted from 511 nm to 490 nm. (Fig. 1)

Absorption and Emission studies for the probe – Cd^{2+} ions

In absorption spectra, initially two peaks are observed for the probe at 273 nm and 332 nm which corresponds to the π-π* and n-π* transitions respectively (Fig.2a). Upon the addition of Cd^{2+}ions, the intensities of absorption peaks at 273nm and 332nm was increased gradually (Fig. 3 a) and they didn't show any remarkable shift. In emission spectra only one peak is observed at 511 nm with the excitation wavelength of 332 nM (Fig.2b). Upon the addition of Cd^{2+} ions, a

new peak is observed at 433 nm with remarkable enhancement of fluorescence intensity (TURN-ON) along with a notable blue shift from the peak at 511 nm. Because, the electron donating ability of the probe is inhibited when Cd^{2+} ions bind with it and the corresponding ICT mechanism is inhibited once again, resulting the blue shift in emission spectra (Fig. 4). In case of fluorescent signaling, molecular switching and metal ions sensing, the Internal Charge Transfer mechanism has been widely exploited owing to its extraordinary spectral shift followed by quantitative detection. Generally, if a fluorophore contains an electron donating group like amino, it undergoes ICT from the donor to the fluorophore upon light excitation, which provides a red-shifted emission. When coordinated with a metal ion, the amino group loses its donating ability. Consequently, the ICT is inhibited and the emission shows blue shift. So that quantum yields always change in the processes. In this chemosensor, triazole part could act as a receptor and the hydroxyl group of the salicyaldimine as ICT donor. An imine group between the receptor and the donor part can induce longer wavelengths in absorption and fluorescence spectra. Hence, the possibility of FRET is ruled out as there is no donor and acceptor separately located in our probe.[29] So the ICT mechanism is followed here. The fluorescence intensity of the new peak at 436 nm is significantly enhanced and the quantum yield is increased from 0.4 to 0.8 with a remarkable blue shift in wavelength. When the concentration of Cd^{2+} ions is gradually increased, the intensity of the emission peak at 436 nm is also increased with a remarkable blue shift from the peak at 511 nm (Fig.3b). The linear range of the developed sensor is varied from 5*f*M to 1*m*M Fig 3b and inset in Fig. 3b show the selective overlay and the corresponding linearity plot with varying the Cd^{2+} ions concentration. For the very first time our simple probe is showed an excellent LOD of 1*f*M. Even for this femto level range a pronounced increased in intensity was observed (Fig. 5)

Calculation of quantum yields (ϕ) by Emission Spectra

Fluorescence quantum yields (ϕ) were estimated from the area under the corresponding fluorescence curves recorded for probe as well as probe-Cd^{2+} ions. The absorbance value of probe was chosen from the absorption spectra (Fig. 2a).The concentration of probe is 5 μM and the integrated area is calculated from the emission spectra of probe and probe-Cd^{2+} ions (Fig. 2b &3) with excitation wavelength of 332 nm in phosphate buffer pH=7.0 . For the standard

Rhodamine 6G, all the values were taken from the previous report. The quantum yield calculation was done based on the following equation.[30, 31]

$$\phi_u = \frac{\phi_s I_u A_s \lambda_{exs} \eta_u}{I_s A_u \lambda_{exu} \eta_s}$$

Where, ϕ is the quantum yield; I is integrated area under the corrected emission spectra; A is absorbance at the excitation wavelength; λ_{ex} is the excitation wavelength; η is the refractive index of the solution; the subscripts u and s refer to the unknown and the standard, respectively. For this study, Rhodamine 6G in Methanol is taken as a standard, which has the quantum yield of 0.91.

Determination of Binding Constant Probe-Cd^{2+} ions Complex

The binding constant K_s of the probe- Cd^{2+} ions are determined in both lower and higher concentration ranges (Fig. 5a and 5b). Benesi-Hildebrand modified equation was used for the calculation of binding constant, where the binding constant was calculated from the ratio of intercept to slope.

K_s= Intercept/ Slope

And it is found to be 2.2 $x10^3$ M^{-1} for femto molar range. From this data, it is clearly revealed that the developed sensor exhibited a very good binding even in lower concentration of Cd^{2+}ions. The stoichiometry of the probe- Cd^{2+} ion is confirmed through a continuous variation method i.e., the Job's Plot.[32] From the figure 6, it is clearly revealed the formation of 1:1 stoichiometry of with a 0.5 molar ratio of probe- Cd^{2+} complex. In addition to that it is also confirmed via the mass spectrometry studies (Fig. S4) and ^{1}H NMR titrations (Fig. S5).

The reversibility experiment was also done by EDTA titration.[33] The initial fluorescence intensity at 436 nm of probe-Cd^{2+} was gradually diminished while vary the EDTA from zero to one equivalent. (Inset Fig. S6). While adding the one equivalent of EDTA to the solution containing probe-Cd^{2+}, the initial fluorescence intensity of the probe at 511 nm is recovered (Fig. S6).These results suggested that the developed sensor could be reusable for real time analysis. [Detailed experimental condition was given in supporting information.] (Scheme 2)

^{1}H NMR titrations of probe-Cd^{2+} ions complex formation

In further, the binding of Cd^{2+} ions with the probe was confirmed by NMR titrations. Upon the addition of 1 equivalent of Cd^{2+} ions to the 1 equivalent of probe, the peak at 10.5 ppm (imine peak) and peak at 3.4ppm (OH) is completely quenched. This study clearly reveals that after the binding of Cd^{2+} ions, the deprotonation takes place. And there is a slight downfield shift experienced by the remaining characteristic peaks which is mainly due to the deshielding effect of the Cd^{2+} ions through the direct N and O-metal interactions (Fig. S5).

Interference studies of other metal ions

The specific selectivity of the probe was also determined by recording the florescent spectra in the presence of series of other metal cations. The interference of other heavy metal ions has studied and observed at the emission peak of Cd^{2+} ion –probe at 436 nm. Expect Cd^{2+} ions, other ions like Au^{3+}, Zn^{2+}, Pb^{2+}, Hg^{2+}, Cr^{3+}, Fe^{2+}, Cu^{2+}, Ca^{2+}, Ba^{2+}, Mg^{2+}, Co^{2+}, Ni^{2+} , Ag^{+}, Na^{+} and K^{+} ions do not show any fluorescence effect at 436 nm. Only the peak intensity at 511 nm slightly decreases for some metal ions without the formation of new peak (Fig. 4). This is due to the formation on non fluorescent complexes with other metal ions. [10, 34] In order to further support, the color changes were observed both visual eye as well as under UV lamp, while the interferents is added to the probe Cd^{2+} ion alone showed an increase in fluorescence when compare to all other interfering metal ions in both visualization.(Fig. S7). Moreover for the Zn^{2+} ions, the synthesized probe has showed an excellent discrimination over Cd^{2+} ions when compare to the other Cd^{2+} ions sensors reported. Under optimized conditions, the developed chemosensor has exhibited a significant enhancement of fluorescence intensity in presence of Cd^{2+} ions. The competitive fluorimetric titrations were also conducted and the results showed a very good selectivity towards Cd^{2+} ions rather than other metal ions. Two types of titrations were done here. Initially 1 equivalent of Cd^{2+} ions (10 μL) was added into the solution of probe (5μM) in the presence of one equivalent of other metal ions. Simultaneously, the same competitive titrations were also carried out with two equivalents of other metal ions (20 μL) (Fig. 7a & 7b). In both the cases, Hg^{2+} ions induce minimal quenching of fluorescence, whereas Li^{+} Ca^{2+} and Na^{+} ions induce a slight enhancement of the fluorescence.

Competitive Spectral Studies in lower concentration (fM) of Cd^{2+} ions

Additionally, the interference of other metal ions were also cross checked for very low concentration of Cd^{2+} ions (*f*M). For this, 1 ml of Cd^{2+} ions (in Femto molar concentration) was added to the 1 ml of probe in the presence of 1 equivalent (10 μL) and two equivalents (20 μL) of other metal ions (Fig. 8a & 8b). In the first test, a Co^{2+} ion has showed a slight increase in fluorescence. Whereas in presence of 2 equivalents of other metal ions, there is a slight increment of fluorescence intensity observed. Hence from these two competitive experiments, it is clearly showed that our probe showed a very good selectivity towards Cd^{2+} ions in a very low concentration (*f*M) in presence of other metals, even in higher concentrations (Fig. 9).

Naked Eye Discrimination of Cd^{2+} from Zn^{2+} ions

As we pointed out early, the discrimination of Cd^{2+} ions from Zn^{2+} ions is very important on cadmium ion based chemosensors. There are many similarities between Cd^{2+} and Zn^{2+} ions. Cd^{2+} ion is commonly found in Zn ores, which are the principal commercial sources of Cd^{2+}. Both metals are classified, commonly with mercury (Hg), in group II B of post-transition elements of the periodic table. Besides, Cd^{2+} ion are intermediate in size between Zn^{2+} and Hg^{2+} ion. $Cd^{2+}$and Zn^{2+} ions have a similar electron configuration on their outer shells. Both metals have filled inner electron shells (d shells) with the outermost shell having two s electrons. Zn^{2+}ion, unlike Cd^{2+} ion is relatively stable in its divalent state and does not undergo redox changes. Cd^{2+} ion is generally classified as a 'soft' metal that is more likely to form covalent linkages with electron-donating ligands, whereas Zn^{2+} ion is classified as 'intermediate in softness.[35] In this developed chemosensor, the binding site i.e. imine nitrogen and hydroxyl group both are coming under soft base categories. So it has selectively binds Cd^{2+} ion (soft acid) rather than Zn^{2+} ion (intermediate base). This phenomenon was also confirmed by the selectivity fluorimetric titrations itself. Moreover, it is clearly distinguished by both naked eye and UV lamp analysis. Initially the probe was colorless under normal vision but it showed an intense green color after the binding of Cd^{2+} ions with the probe. The same trend was also observed when the probe is subjected to UV lamp. The slight green fluorescence color of the probe is increased immensely (very bright green fluorescence) after the addition of Cd^{2+} ions (Fig.10a & 10b). In both the visualization, Zn^{2+} ions have showed only a negligible change. So our synthesized fluorophore is successfully discriminates the Cd^{2+} ions from the Zn^{2+} ions in both naked eye and under UV Lamp.

Imaging studies at Living cells

To further highlight the practical application of the probe, we carried out living cells imaging studies by using the confocal fluorescence microscopy. Incubation of He-La cells with probe (5 μM) for 0.5 h at 37 °C was followed by the addition of Cd^{2+} ions (5 μM) and then was incubated for another 0.5 h. Initially the cell exhibits a moderate weak fluorescence and then the great enhancement of fluorescence is observed (Fig. 11).These results are suggested that the ability of the probe to penetrate the cell membrane and can be used for tracking the of Cd^{2+} ions in living cells and in vivo potentially.

Conclusion

In conclusion, we have designed a new simple fluorescent sensor platform based on the simple salicyaldimine based fluorophore. It shows high sensitivity in femto level and selectivity toward Cd^{2+} ion in physiological pH. The fluorescence intensity was significantly enhanced and the quantum yield was increased from 0.4 to 0.8. Moreover, its fluorescence intensity is enhanced in a linear fashion with lower concentration (*f*M) of Cd^{2+} ion and thus can be potentially used for quantification of Cd^{2+} ion even it will present in femto molar concentration. The living cell imaging studies under physiological pH further demonstrate its value in the practical applications of biological systems.

Acknowledgement

This work is financially supported by DST-INSPIRE Fellowship Scheme, NEW DELHI, INDIA. So, the author thanks DST for offering fellowship for pursuing his Ph.D program.

Abbreviations

PET- Photoinduced Electron Transfer, ICT- Internal Charge Transfer, FRET- Fourier Energy Transfer, CHEF- Chealtion Enhanced Fluorescence.

References

(1) (a) G. K.Walkup and B. Imperiali, *J. Am. Chem. Soc.,* 1996, **118**, 3053. (b) Liu, J.; Lu, Y. *J. Am. Chem. Soc.,* 2004, **126**, 12298.

(2) (a) S. Deo and H. A. Godwin, *J. Am. Chem. Soc.,* 2000, **122**, 174. (b) J. Li, Y. Lu, *J. Am. Chem. Soc.,* 2000, **122**, 10466.

(3) (a) A. Miyawaki, J. Llopis, R. Helm, J. M. McCaffery, J. A. Adams, M. Ikura, R. Y. Tsien, *Nature.,* 1997, **388**, 882. (b) P. Chen, C. He, *J. Am. Chem. Soc.,* 2004, **126**, 728.

(4) (a) H. Wang, L. Xue, H. Jiang, *Org. Lett.,* 2011**, 13**, 3844. (b) P. N. Basa, A. Bhowmick, M. M. Schulz, A. G. Sykes, *J. Org. Chem*., 2011, **76**, 7866. (c) A. E. Palmer, *ACS Chem. Biol*., 2009, **3**, 157. (d) J. H. Lee, A. R. Jeong, I. S. Shin, H. J. Kim, J. I. Hong, *Org. Lett.,* 2010**, 12**, 764. (e) M. Zheng, Z. Xie, D. Qu, D. Li, P. Du, X. Jing, Z. Sun, *ACS Appl. Mater*. *Interfaces.,* 2013, **5**, 13242. (f) R. R. Lauwerys, A. M. Bernard and H. A. Reels, *Clin. Chem*., 1994, **40**, 1391. (g) T. Jin, J. Lu, M. Nordberg, *Neurotoxicology.,* 1998, **19**, 529. (h) Agency for Toxic Substances and Disease Registry, 4770 Buford Hwy NE, Atlanta,GA 30341. http://www.atsdr.cdc.gov/cercla/07list.html.

(5) (a) R. E. Clement, P. W. Yang, C. Koester, J. *Anal. Chem.,* 1999, **71**, 257.

(b) L. H. Thaller, A. H. Zimmerman, *J. Power Sources.,* 1996, **63**, 53.

(c) R. E. Hamon, M. J. McLaughlin, R. Naidu, R. Correll, *Environ. Sci.Technol.,* 1998, **32**, 3699.

(d) S. E. Bailey, T. J. Olin, R. M. Bricka, D. D. Adrian, *Water Res.,* 1999, **33**, 2469.

(6) (a) M. P. Waalkes, *J. Inorg. Biochem.,* 2000, **79**, 241.

(b) M. P. Waalkes, T. P. Coogan, R. A. Barter, *Crit. Rev. Toxicol.,* 1992, **22**, 175.

(c) W. de Vries, P. F. Römkens and G. Schütze, Rev. Environ. Contam. Toxicol., 2007, **191**, 91. (d) H. N. Kim, W. X. Ren, J. S. Kim and J. Yoon, Chem. Soc. Rev., 2012, 3210 and references therein.

(7) (a) C. Cloquet, J. Corrigan, G. Libourel, T. Sterckeman, E. Perdrix, *Environ. Sci. Technol.,* 2006, **40**, 2525. (b) S. P. Dolan, D. A. Nortrup, P. M. Bolger, S. G. Capar, S. G. *J. Agric. Food Chem.,* 2003, **51**, 1307.

(8) (a) N. H. Bings, A. Bogaerts, J. A. C. Broekaert, *Anal. Chem.,* 2002, **74**, 2671. (b) S. M. Pyle, J. M. Nocerino, S. N. Deming, J. A. Palasota, J. M. Palasota, E. L. Miller, D. C. Hillman,

C. A. Kuharic, W. H. Cole, P. M. Fitzpatrick, M. A Watson, K. D. Nichols, K. D. *Environ. Sci. Technol.,* 1996, **30**, 204.

(9) (a) Y. Wang, Y. H. Wang, Z. L. Fang, *Anal. Chem.,* 2005, **77**, 5396. (b) Q. Y. Ye,Y. Li, Y. Jiang, X. P. Yan, *J. Agric. Food Chem.,* 2003, **51**, 2111.

(10) (a) K. Komatsu, Y. Urano, H. Kojima, T. Nagano, *J. Am. Chem. Soc.* 2007, **129**, 13447.(b) E. M. Nolan, S. J. Lippard, *J. Am. Chem. Soc.,* 2007, **129**, 5910. (c) S. Yoon, A. E. Albers, A. P. Wong, C. J. Chang, *J. Am. Chem. Soc.,* 2005, **127**, 16030. (d) J. Y. Kwon, Y. J. Jang, Y. J. Lee, K. M. Kim, M. S. Seo, W. Nam, J. Yoon, *J. Am. Chem. Soc.,* 2005, **127**, 10107. (e) J. Wang, X. Qian, J. Cui, *J. Org. Chem.,* 2006, **71**, 4308. (f) X. Guo, X. Qian, L. Jia, *J. Am. Chem. Soc.,* 2004, **126**, 2272. (g) C. Lu, Z. Xu, J. Cui, R. Zhang, X. Qian, *J. Org. Chem.,* 2007, **72**, 3554. (h) M. Royzen, Z. Dai, J. W. Canary, *J. Am. Chem. Soc.,* 2005, **127**, 1612. (i) W. Jiang, Q. Fu, H. Fan, J. Ho, W. Wang, *Angew. Chem., Int. Ed.,* 2007, **46**, 8445. (j) C. W. Rogers, M. O. Wolf, *Angew. Chem., Int. Ed.,* 2002, **41**, 1898. (k) A. Coskun, E. U. Akkaya, *J. Am. Chem. Soc.,* 2006, **128**, 14474. (l) J. F. Callan, A. P. de Silva, D. C. Magri, D. C. *Tetrahedron.,* 2005, **61**, 8551.

(11) C. Lu, Z. Xu, J. Cui, R. Zhang, X. Qian, *J. Org. Chem.,* 2007, **72**, 3554.

(12) J. Jia, Q. C. Xu, R. C. Li, X. Tang, Y. F. He, M. Y. Zhang, Y. Zhang, G. W. Xing, G. *Org. Biomol. Chem.,* 2012, **10**, 6279.

(13) W. Wang, Q. Wen, Y. Zhang, X. Fei, Y. Li, Q. Yang, X. Xu, *Dalton Trans*., 2013, **42**, 1827.

(14) (a) F. A. Cotton and G. Wilkinson, *Advances in Inorganic Chemistry.*, 5th ed.; Wiley: New York., 1988, 957. (b) D. Dakternieks, *Coord. Chem. Rev.,* 1990, ***98***, 279. (c) M. Li, H. Y. Lu, R. L. Liu, J. D. Chen, C. F.Chen, *J. Org. Chem.,* 2012, **77**, 3670.

(15) A. Bencini, F. Caddeo, C. Caltagirone, A. Garau, M. B. Hurstouse, F. Isaia, S. Lampis,V. Lippolis, F. Lopez, V. Meli, M. Monduzzi, M. C. Mostallino, S. Murgia, S. Puccioni, J. Schmidt, P. P. Seccif, Y. Talmong, *Org. Biomol. Chem.,* 2013, **11**, 7751.

(16) L. Xue, C. Liu, H. Jiang, *Org. Lett.,* 2009**, 11**, 1656.

(17) R. T. Bronson, D. J. Michaelis, R. D. Lamb, G. A. Husseini, P. B. Farnsworth, M. R. Linford, M. R. M. Izatt, J. S. Bradshaw, P. B. Savage, *Org. Lett.,* 2005**, 7**, 1106.

(18) S. Sarkar, R. Shunmugam, *Appl. Mater. Interfaces***.,** 2013, **5**, 7379.

(19) L. Xue, C. Liu, H. Jiang, H. *Org. Lett.,* 2009, **11**, 1655.

(20) L. K. Zhang, Q. X. Tong, L. J. Shi, *Dalton Trans.,* 2013, **42**, 8567.

(21) C. Lu, Z. Xu, J. Cui, R. Zhang, X. Qian, *J. Org. Chem.,* 2007, **72**, 3554.

(22) X. Peng, J. Du, J. Fan, J. Wang, Y. Wu, J. Zhao, S. Sun, T. J. Xu, *J. Am. Chem. Soc.,* 2007, **129**, 1500.

(23). T. Cheng, Y. Xu, S. Zhang, W. Zhu, X. Qian, L. Duan, *J. Am. Chem. Soc.,* 2008, **130**, 16160.

(24). X. Liu, N. Zhang, J. Zhou, T. Chang, C. Fangab, D. Shangguan, *Analyst.,* 2013**, 138**, 901.

(25). P. G. Sutariya, A. Pandya, N. R.Modi, S. K. Menon, *Analyst.,* 2013, **138**, 2244.

(26). M. Taki, M. Desaki, A. Ojida, S. Iyoshi, T. Hirayama, I. Hamachi, Y. Yamamoto, *J. Am. Chem. Soc.,* 2008, **130**, 12564.

(27). F. Robert, A. D. Naik, F. Hidara, B. Tinant, R. Robiette, J. Wouters, Y. Garcia, Y. *Eur. J. Org. Chem.,* 2010, **10**, 621.

(28). R. Herchel, L. Pavelek, Z. Tr´avn´ıˇcek, *Dalton Trans.,* 2011, **40**, 11896.

(29). C. Kaewtong, J. Noiseephum, Y. Uppa, N. Morakot, N. Morakot, B. Wanno, T. Tuntulani, B. Pulpoka, *New J. Chem.,* 2010, **34**, 1104.

(30). D. Magde, R. Wong, P. G. Seybold, *Photochemistry and Photobiology.*, 2002, **75**(4), 327.

(31). (a) C. Tanyu, X. Yufang, Z. Shenyi, Z. Weiping, Q. Xuhong, D. Liping, *J. Am. Chem. Soc*., 2008, **130**, 16160. (b) J. R. Lakowicz, *Principles of Fluorescence Spectroscopy*, second edition, Kluwer Academic/Plenum, 1999, 725 pp. (c) M. Fischer and J. Georges, *Chemical Physical Letters*., 1996, **260,** 115.

(32). (a) J. Hatai, S. Pal, S. Bandyopadhyay, *Tetrahedron Lett.*, 2012, **53**, 4357. (b) C.Alexander, F. M Mary, A. De Bank. Paul, C. Lorenzo, *Org. Biomol. Chem*., 2012, **10**, 8753. (c) G. S. Pinkesh, R. M. Nishith, P. Alok, K. J. Bhoomika, V. J. Kuldeep, K. M. Shobhana, *Analyst*., 2012, **137**, 5491. (d) W. Wei, W. Qian, Z. Yue, F. Xiaoliang, L. Yaoxian, Y. Qingbiao Yang, X. Xiaoyi Xu, *Dalton Trans*., 2013, **42**, 1827.

(33). S. Muthaiah Shellaiah, W. Yen-Hsing, L. Hong-Cheu, *Analyst*, 2013, **138**, 2931.

(34). (a) M. Hiroshi, S. Hiroshi, S. Tokashi, H. Kei, Y. Seikichi, M. Noboru, *J. Phys. Chem.* 1984**,88,** 5868. (b) S. T. Samuel, J. K. Su, T. K. Eric, *J. Am. Chem. Soc*., 2011, **133**, 2664. (c) Y. P.

Sun, H. Y. Jung Hee, S. H. Chang, S. Rachid, S. K. Jong, E. M. Susan, V. Jacques, *J. Org. Chem.* 2008, ***73***, 8212.

(35). K. B. Jacobson, J. E. Turner, J.E., 1980. *The interaction of cadmium and certain other metal ions with proteins and nucleic acids.* Toxicology **16**, 1.

Schemes

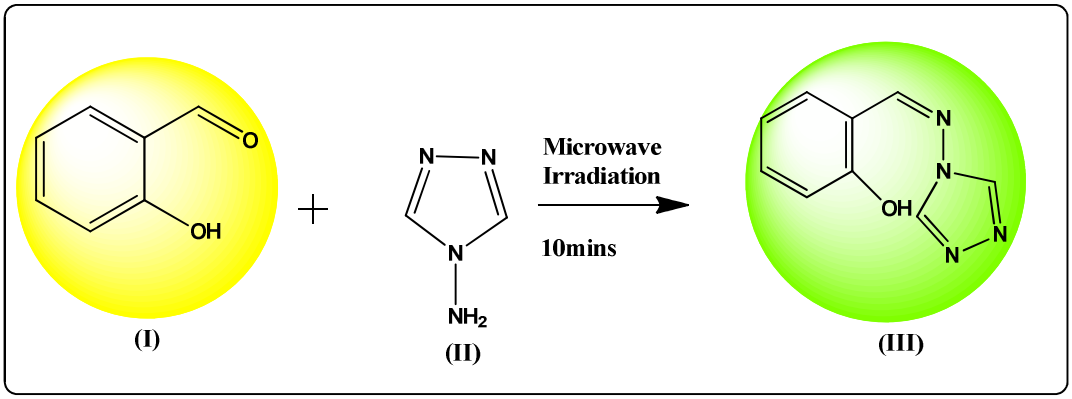

Scheme 1 Synthesis of the probe [(Z)-2-(4H-1, 2, 4-triazol-4-yl) imino methylphenol]

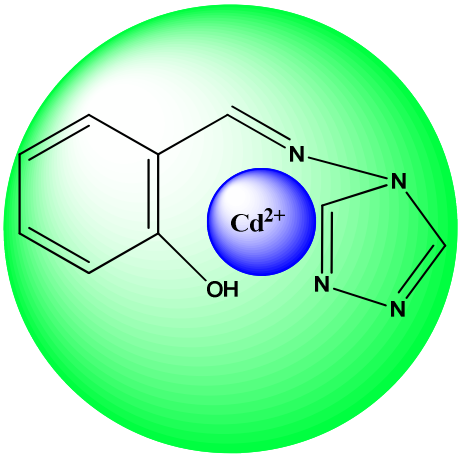

Scheme 2 Development of the chemosensor probe [(Z)-2-(4H-1, 2, 4-triazol-4-yl) imino methylphenol] – Cadmium ions (II)

Table

Sl.No	Type of the Chemosensor	Mechanism	Selectivity	Sensitivity	Quantum yield	Reference
1.	OFF - ON	CHEF	Cd^{2+}	53nM	---	14
2.	TURN ON	PET	Cd^{2+}	0.25 + 0.03 pM	0.2	15
3.	TURN ON	PET	Cd^{2+}	1.6nM	0.3	17
4.	TURN ON	ICT	Cd^{2+}	0.1 µM	0.6	21
5.	TURN ON	PET	Cd^{2+}	0.6µM	0.3	23
6.	TURN ON	PET	Cd^{2+}	48 nM	---	24
7.	ON-OFF-ON	PET	Cd^{2+} Sr^{2+}	0.94pM	---	25
8.	TURN ON	ICT	Cd^{2+}	100pM	0.7	26
9.	TURN ON	ICT	Cd^{2+}	1fM	0.8	In this work

Table 1 Various types of Cd^{2+} ions sensors and their lower limit of detection.

Figures

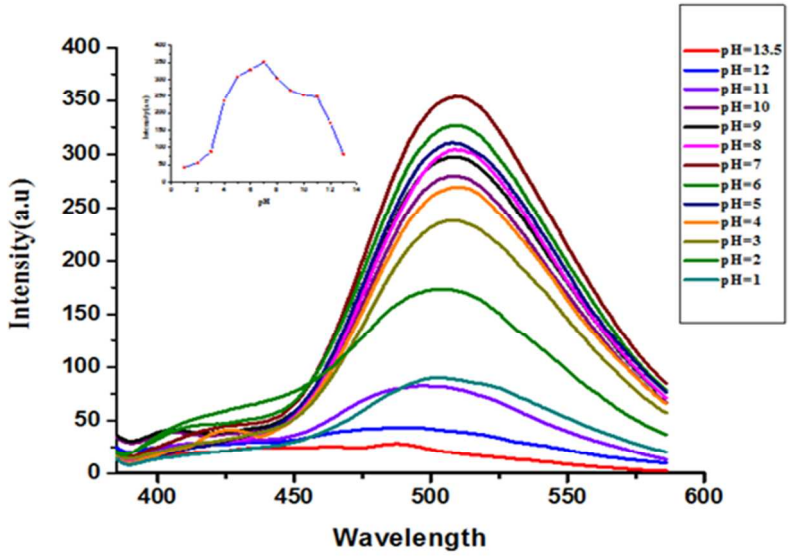

Fig. 1 Effect of pH on fluorescence Intensity of sensor in buffer (pH=7.0). The concentration of probe is 5 µM, excitation wavelength was 332nm. Emission spectra of probe at pH from 1 to 13.5 [Inset: Fluorescence Intensity at 511 nm versus pH. Excitation and emission slit widths are 5 nm and 2.5 nm respectively].

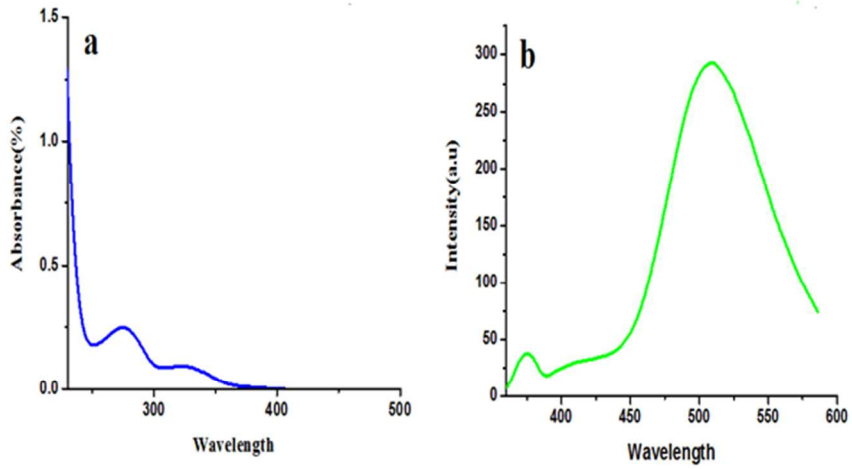

Fig. 2 (a) Absorption spectra and (b) Emission spectra [with excitation wavelength of 332 nm in phosphate buffer pH=7.0) concentration of probe is 5 µM].

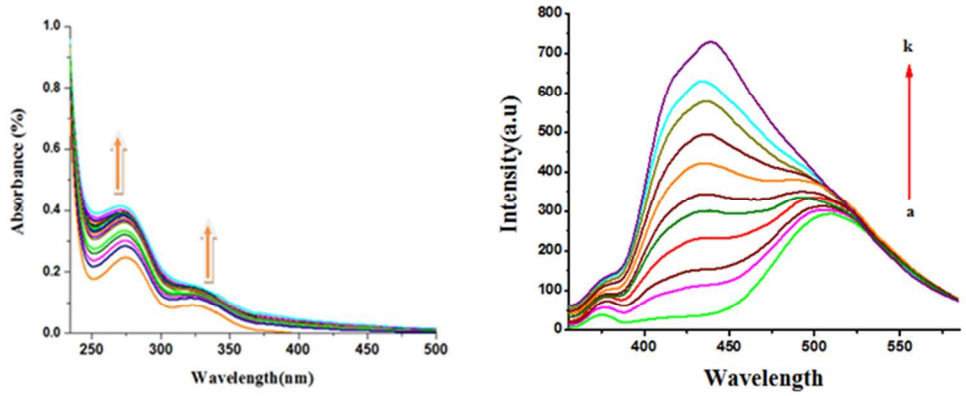

Fig. 3 (a) Absorption spectra of the probe in presence of Cd^{2+} ions from 0-20μM and (b) Emission spectra with excitation wavelength of 332 nm in phosphate buffer (pH=7.0) in the presence of increasing the concentration of Cd^{2+} ions from ($5x10^{-15}$M to $1x10^{-3}$M). (a) probe; (b) $5x10^{-15}$ (c) $1x10^{-14}$; (d) $1x10^{-12}$: (e) $1x10^{-9}$; (f) $5x10^{-9}$; (g) $1x10^{-8}$; (h) $1x10^{-6}$: (i) $5x10^{-6}$; (j) $1x10^{-5}$; (k) $1x10^{-3}$.The concentration of the probe is 5 μM. [Excitation and emission slit widths are 5 nm and 2.5 nm respectively Inset: corresponding linearity plot for the selective concentrations].

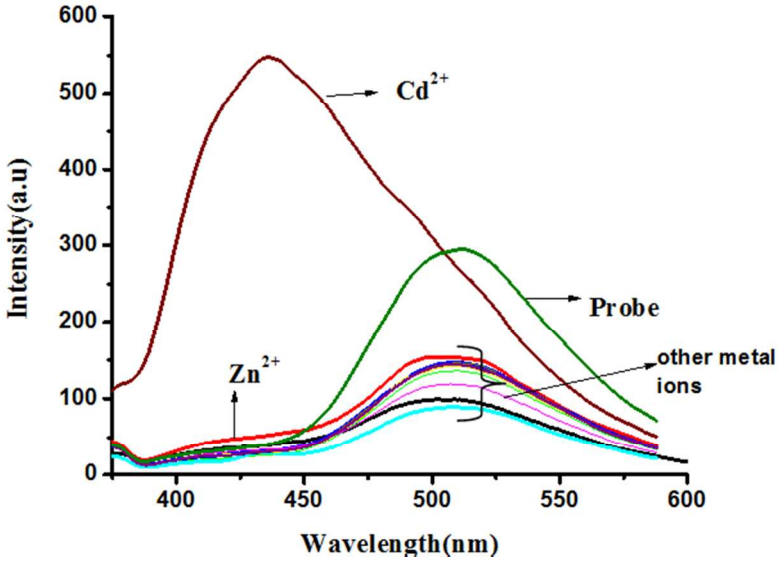

Fig. 4 Selectivity of probe in phosphate buffer (pH = 7.0) in the presence of different metal ions. Excitation wavelength is 332 nm In this emission plot, Zn^{2+} ions and other metal ions are quenches the fluorescence intensity of the probe with little change in the emission maximum but enhancement with enormous blue shift is only observed in the presence of Cd^{2+}ions. [The total concentration of sensor is 5 μM. Excitation and emission slit widths are 5 and 2.5 nm respectively].

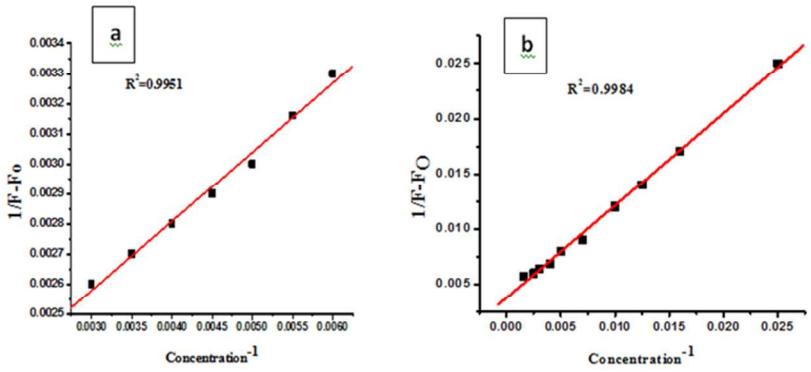

Fig. 5 (a) Linear response of Sensor as a function of higher concentration of Cd^{2+} ions in buffer solution (pH=7.0). (b) Linear response of Sensor as a function of lower concentration of Cd^{2+} ions (fM) in buffer solution (pH=7.0).

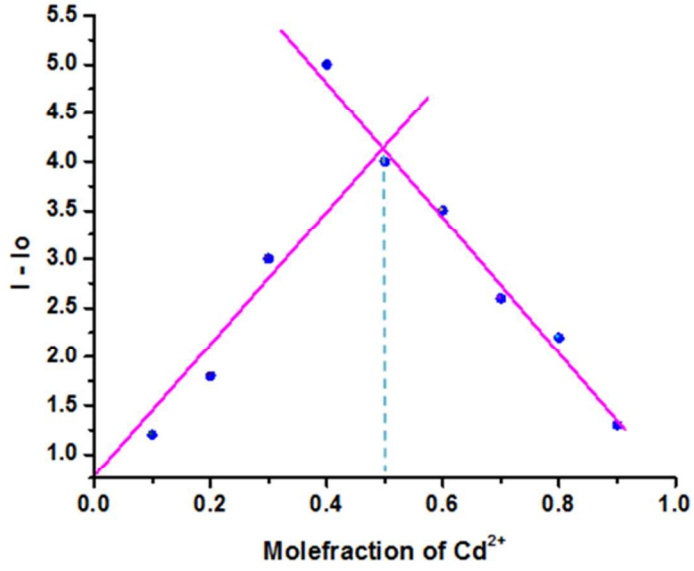

Fig. 6 Job's Plot of probe (1.0 equiv) in presence of Cd^{2+} ions (1.0 equiv). [Confirms the formation of 1:1 complex of Probe-Cd^{2+} ion]

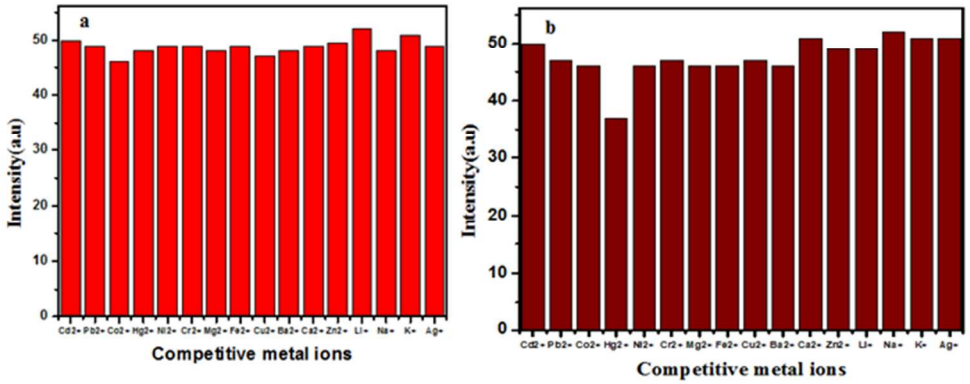

Fig. 7 (a) The fluorescence intensity of sensor at 511 nm with 1 equiv (10 µL) of other metal ions followed by 1 equiv Cd^{2+}ions (10 µL) (b) Fluorescence intensity of sensor at 511 nm with 2 equiv (20 µL) of other metal ions followed by1 equiv Cd^{2+}ions (10 µL). [Concentration of probe is 5 µM, Phosphate buffer, pH 7.5 and Slit widths were 5 nm and 2.5nm respectively. Excitation wavelength is 332 nm, concentration of Cd^{2+} ions and other metal ions are $1X10^{-3}$ M)

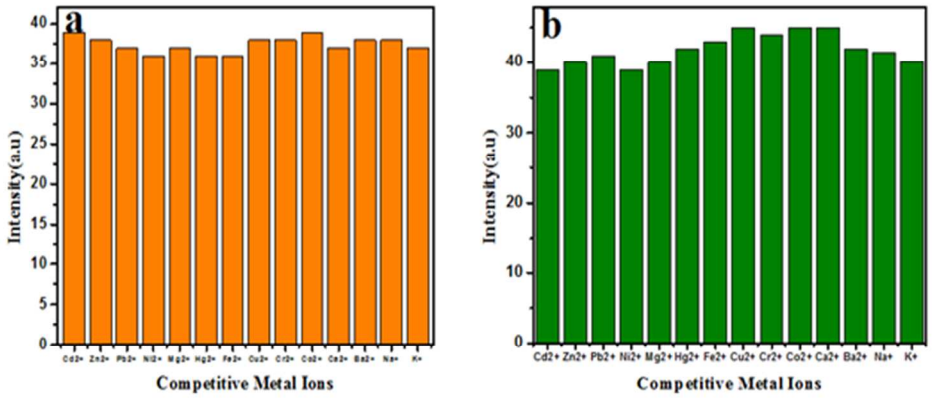

Fig. 8 (a) Fluorescence intensity of 1ml of probe with 1 ml of Cd^{2+} ions in presence of one equivalent (10 µL) of other metal ions. (b) Fluorescence intensity of 1ml of probe with 1 ml of Cd^{2+} ions with 2 equivalents (20 µL) of other metal ions. [Excitation wavelength 332 nm in phosphate buffer solution (pH=7.0), excitation and emission slit widths are 5 nm and 2.5 nm respectively, the concentration of other interfering metal ions are$1x10^{-3}$M and Cd^{2+} ions are $1x10^{-15}$M]

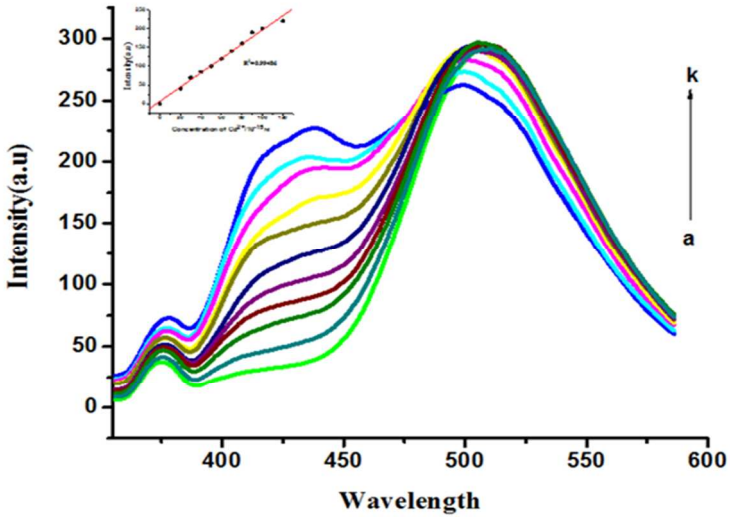

Fig. 9 Emission spectra of probe in the presence of lower concentrations of Cd^{2+} ions. [Inset: Fluorescence intensity of probe (5 µM) at 436 nm as a function of concentration of Cd^{2+} ions $1x10^{-15}$ M to $5x10^{-12}$ M in buffer solution (pH=7.0). Excitation and emission slit widths are 5 nm and 2.5 nm, respectively.] (a) probe; (b) $1x10^{-15}$ (c) $2x10^{-15}$; (d) $3x10^{-15}$: (e) $5x10^{-15}$; (f) $1x10^{-14}$; (g) $5x10^{-14}$; (h)$1x10^{-13}$; (i) $5x10^{-13}$; (j) $1x10^{-12}$ and (k) $5x10^{-12}$.

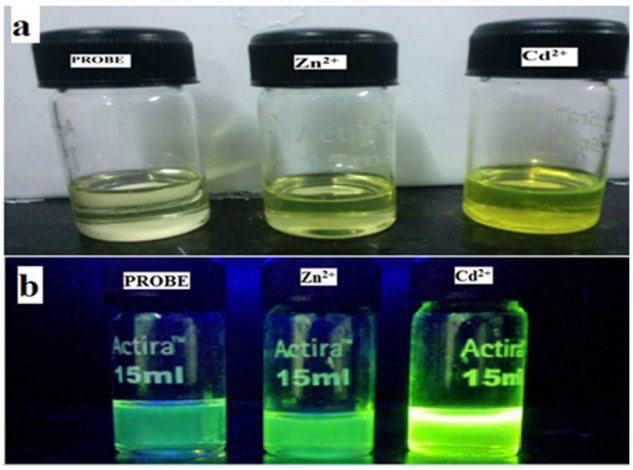

Fig. 10 (a) Naked eye detection of Cd^{2+} over Zn^{2+}ions and (b) Response of the probe in presence of Cd^{2+} ion under UV-Lamp.

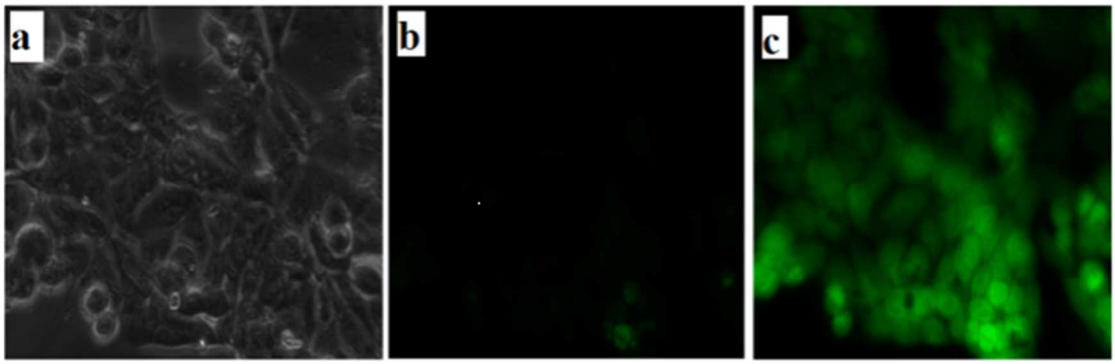

Fig.11. Fluorescent images of Cd^{2+} ions in HeLa cells. (a) Bright-field transmission image of HeLa Cells incubated with probe (5 µM). (b) Fluorescence image of HeLa cells incubated with probe (5 µM). (c) Fluorescence image of HeLa cells incubated with probe for 30 min, washed three times, and then further incubated with 5 µM Cd^{2+} ions for 30 mins.